ADVANCED ELECTRICAL AND OPTICAL DIAGNOSTICS ON ATMOSPHERIC PRESSURE PLASMAS WITH FOCUS ON MICRODISCHARGES

K.-D. WELTMANN[1]*, T. GERLING[1], H. HÖFT[1], T. HODER[1], A. PIPA[1], A. V. NASTUTA[2], R. BRANDENBURG[1], R. BUSSIAHN[1], M. KETTLITZ[1]

[1] INP Greifswald (Leibniz Institute for Plasma Science and Technology), D-17489 Greifswald, Germany
[2] Faculty of Physics, Alexandru Ioan Cuza University, 700506 Iasi, Romania
*weltmann@inp-greifswald.de

ABSTRACT

The application of non-thermal atmospheric pressure plasmas in emerging fields like plasma medicine, decontamination, surface and water treatment, and pollutant degradation of gases requires the profound knowledge on its parameters and properties. The investigation of such plasmas is a challenging task since most of these plasmas are transient and filamentary. The contribution summarizes experimental methods for the electrical, optical and spectroscopic diagnostics on barrier microdischarges, self-pulsing transient spark discharges and RF-driven capillary plasma jets with suitable temporal and spatial resolution in order to demonstrate the peculiarities and limitation of methods being described (e.g. ICCD imaging, streak camera recording, cross-correlation spectroscopy, phase-resolved optical emission spectroscopy).

1. INTRODUCTION

Within the last two decades an increasing interest on plasmas operated at open atmospheres can be asserted. Beside the established technologies (ozone generation, surface "corona" treatment) the fields of therapeutic applications or pollutant degradation in gas streams have emerged. In this branch of study dielectric barrier discharges (DBDs) and atmospheric pressure plasma jets (APPJs) are often considered [1, 2]. Examples are given in the figure 1.

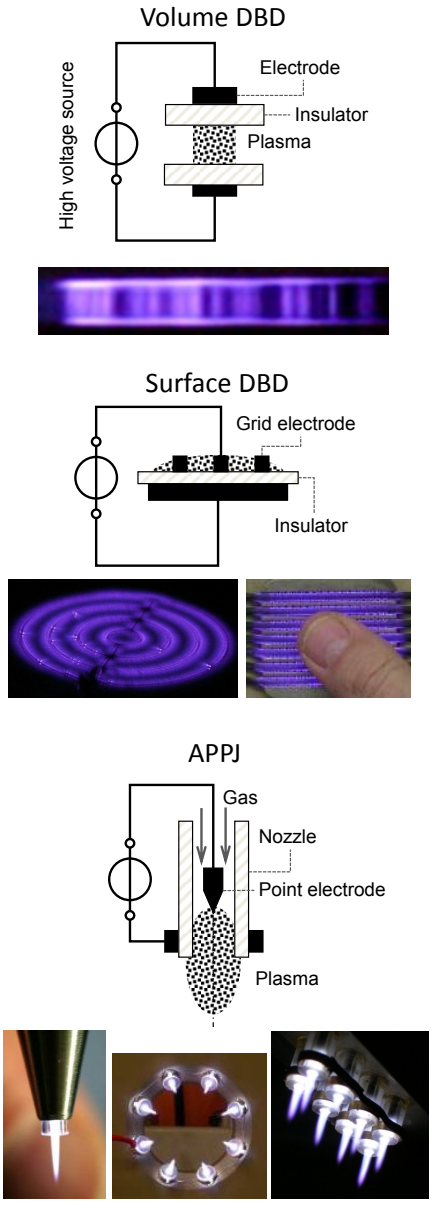

Fig. 1: *Examples of plasma sources operating at open atmospheres*

The generation and control of non-thermal plasmas at atmospheric pressure is a challenge for the design and construction. For information on the discharge development it is necessary to get insights on the elementary processes, to benchmark simulation results of such plasmas and to enable the determination of basic plasma parameters.
Non-thermal plasmas in reactive gases are usually transient, small-sized, non-uniform and filamentary, i.e. consisting of distinct, constricted discharge channels (see photos in figure 1). Nowadays a broad spectrum of plasma diagnostic methods is available [3]. This contribution will give an overview of the capabilities for the electrical, optical and spectroscopic diagnostics, which are demonstrated on three different plasma sources. The techniques provide the necessary time resolution, are non-intrusive and give insights on the plasma morphology and its spatially and temporally resolved development. The plasma sources being discussed are (1) single barrier microdischarges in nitrogen-oxygen gas mixtures operated by rectangular high voltage, (2) a self-pulsing DC spark discharge in flowing argon at open air, and (3) an AC operated needle-to-plane discharge in flowing helium at open air.

2. SINGLE DIELECTRIC BARRIER MICRODISCHARGES

The discharge being investigated is shown in figure 2 (a). Single repetitive microdischarges are generated in a symmetric electrode arrangement with semi-spherical electrodes [4]. The dielectric is alumina (Al_2O_3) with a thickness of about 0.5 mm. The minimum distance between the electrodes amounts to 1 mm. The electrodes are located in a gas cell made of Plexiglas. Thus a defined gas mixtures can be flushed through the cell (total flow rate 100 sccm).
Electrical measurements (current, applied voltage) are performed with fast probes (Tektronix CT-1 and P6015A) and recorded with a digital sampling oscilloscope (Tektronix TDS 7054 with 5 GS/s, 500 MHz bandwidth). In our DBD arrangement the current probe is directly embedded in one of the electrodes which reduces stray capacitances and inductances [4]. Measured current and voltage signals are shown in figure 2 (c). The applied voltage is of rectangular shape with a rise time of 250 V/ns and an amplitude of 10 kV.

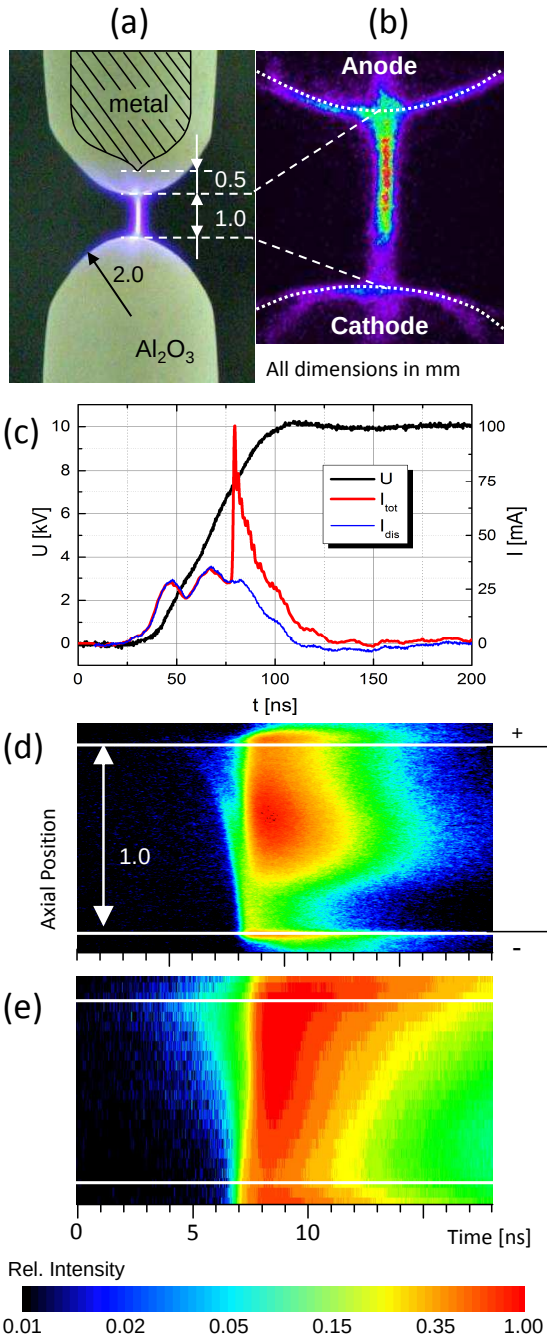

Fig. 2: Investigation of single microdischarges (a) by means of ICCD camera recording (b), current and voltage measurements (c), streak camera (d) and CCS at a wavelength of 337 nm (e). Results are for the rising slope of a unipolar rectangular high voltage (repetition frequency 10 kHz) in N_2 with 0.1 vol.% O_2 admixture [10].

The measured total current I_{tot} consists of the displacement current I_{dis} and the plasma induced (discharge) current. The displacement current can be obtained from the derivation of the applied voltage (scaled with the total capacitance) or can be measured, when no microdischarge is ignited (which is often the case when starting the discharge after a certain off time of non-operation). The plasma induced current is obtained by sub-

traction of I_{dis} from I_{tot} and multiplication with the factor $C_{\mathrm{b}}/(C_{\mathrm{b}} - C_{\mathrm{tot}})$, where C_{b} is the capacitance of the dielectric barriers and C_{tot} is the capacitance of the total DBD arrangement [5, 6, 7].
The determination of the electrical parameters of DBDs (plasma induced current, dissipated energy and power, capacitances) is based on an equivalent circuit. The simplest equivalent circuit suitable in most situations including the classical ozonizer and uniform DBDs in small scale laboratory reactors consists of a capacitance representing the dielectric barrier in series with a parallel connection of a variable resistor and a gas gap capacity. This parallel connection is capable to cover the change of the effective capacitance and non-zero gas gap voltage during discharge ignition. This is particularly the case for pulsed operated DBDs when the applied voltage changes during the breakdown and the active plasma phase [6, 8].

The microdischarges are either investigated simultaneously by a fast ICCD camera and a streak camera system by using a beam splitter or by means of cross-correlation spectroscopy (CCS). With the ICCD camera it is possible to record images of single microdischarges (resolution: $\Delta\mathrm{t} \geq 2\,\mathrm{ns}$, $\Delta\mathrm{x} \geq 2\,\mu\mathrm{m}$), while streak photos yield the spatio-temporal development of microdischarges along its axis centerline ($\Delta\mathrm{t} \geq 50\,\mathrm{ps}$, $\Delta\mathrm{x} \geq 2\,\mu\mathrm{m}$). CCS is based on sensitive time-correlated single photon counting and thus the most sensitive method, which also enables spectrally selected investigation [9]. Spatial resolution of $10\,\mu\mathrm{m}$ and time resolution of up to $10\,\mathrm{ps}$ can be reached [4, 10]. In figure 2 (b-d) results of ICCD recording, streak camera measurements, and CCS for the most intensive emission in the optical emission spectrum (0-0 transition of the second positive system of N_2) are compared.
The ICCD camera photo in figure 2 (b) is for an individual microdischarge. It expands in the gas gap (diameter about 75 µm [7]) towards the electrodes and spread into several discharge channels on the dielectric surfaces. Both, streak and CCS figures (2 (d) and (e)) reveal the spatio-temporal development of repetitive microdischarges. In these figures the axial coordinate is the ordinate, while the abscissa is the time scale (which is relative). The number of counted photons is color coded in logarithmic scale. The streak camera enables in principle the recording of the discharge development of individual microdischarges, while the CCS plot is always the result of an accumulation of signal over many discharge cycles (usually in the range of 10^6). However, under the conditions being considered the accumulation over about 10^3 microdischarges is necessary in order to get a more clear picture of discharge development [10]. One needs to be careful with signal accumulation with such techniques. In our case the simultaneous use of streak camera, electrical measurements and ICCD imaging allows to exclude recordings of multiple microdischarges and to check the reproducibility as well as the stability of spatial localization. This could be confirmed for these experiments [4]. Furthermore, the streak camera system handles a temporal jitter of the microdischarges by means of a sophisticated image processing (jitter correction function) [10].
The advantage of CCS is the high sensitivity which is beneficial, e.g. if studying the weak pre-phase of microdischarge development or in case of spectrally resolved measurements of low signals. Furthermore, CCS enables the recording of the discharge development in case of erratic appearing microdischarges as in case of sinusoidal operated DBD [9]. However, in case of pulsed operated barrier microdischarges modern streak cameras distinguish with much lower signal accumulation times but a reasonable dynamic range and sensitivity. Thus it is well suited to get a systematic overview on the discharge development in a wide range of operation parameters while CCS should be applied for the investigation of specific aspects under selected conditions [10].

3. SELF-PULSING TRANSIENT SPARK

The self-pulsing transient spark discharge is shown in figure 3 (a) [11]. It is operated by negative DC voltage (-5 to -10 kV) applied by a high resistive power supply on a hollow needle electrode (0.8 mm outer diameter, 0.6 mm inner diameter). A grounded copper plate ($4 \times 4\,\mathrm{cm}^2$) as the counter electrode is placed about 8 mm apart from the needle tip. A quartz capillary surrounds the needle electrode and is usually placed 5 mm from the needle tip. An argon gas flow rate between 0.2 and 0.5 slm is supplied through the needle electrode. An argon gas channel forms in front of the outlet, which increasingly mixes with ambient air.

A transient single discharge filament with a diameter of 60 µm is created. The self-pulsing effect with short discharge duration is caused by high resistivity and consequently limited power load.

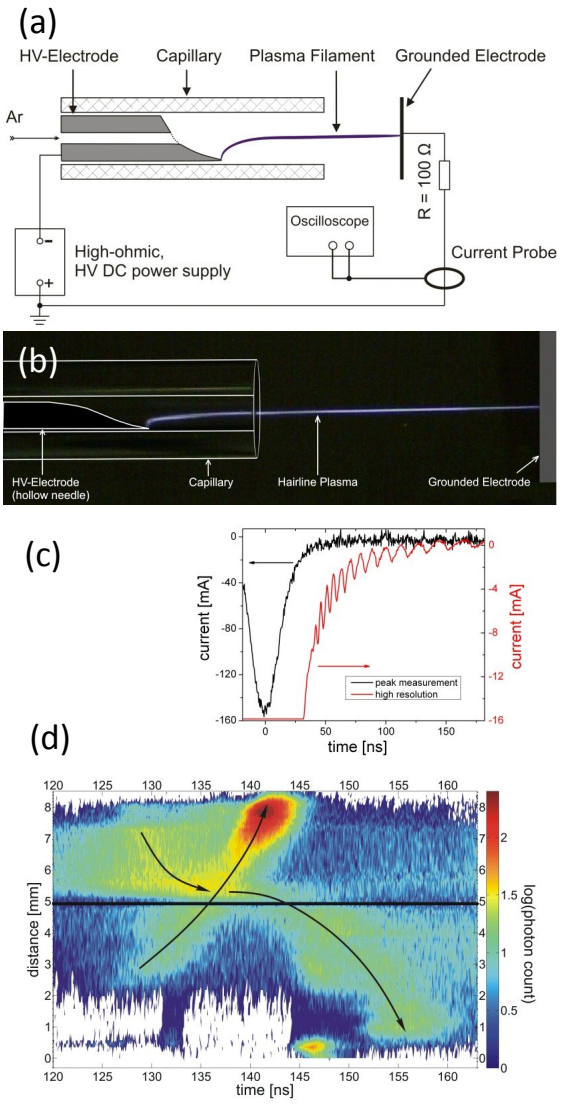

Fig. 3: *Investigation of the self-pulsing transient spark: (a) Electrode arrangement and improved set-up for electrical measurements, (b) Photo of the plasma source with reworked electrode arrangement, (c) Results of electrical characterization, (d) CCS result at wavelength of 337 nm. [13, 14].*

In our first studies, the current was measured as the voltage drop over a 100 Ω resistor attached to the grounded electrode and the voltage was measured capacitively by a high voltage probe (Tektronix P6015A) mounted in open air close to the discharge (used as an antenna to avoid voltage divider circuit, see [12]). The repetition frequency of the discharge channels varies between 0.5 and 3 kHz while typical discharge current amplitudes between 0.1 A and 2 A are observed. A typical current pulse is shown in figure 3 (c). The plasma is characterized as a transient spark discharge with a duration of about 30 ns (FWHM about 10 ns). The discharge repetition rate is dependent on the applied voltage amplitude, the gas flow rate, and the dimensions of the electrode arrangement. This overall electrical behavior can be described utilizing an equivalent circuit representing the plasma channel as a series of impedances, each of them determined by a resistance and a capacitance [13]. The first experiments reveal strong, long-lasting oscillations in the discharge current signal. More detailed studies on the influence of operating conditions on these oscillations show a strong effect of ground loops. Employing the single current probe (Tektronix CT1 connected to two channels of the oscilloscope (Tektronix DPO 7104)), without doing voltage measurements at the same time the measurements are unaffected from variable cable lengths or grounding conditions. Even with this set-up current oscillations with decreasing frequency between 250 MHz and 50 MHz are observed in a specific gas flow range. A further analysis has shown that this behavior can be interpreted as the propagation of ion acoustic waves in the discharge channel. From the observed oscillation frequencies, Ar_2^+ ion densities can be determined [14].

Since the transient spark discharge channels appear quite irregular streak camera recording or gated ICCD camera recording cannot be applied to study the discharge development with high time resolution. Therefore CCS ($\Delta t \geq 80$ ps, $\Delta x \geq 100$ µm) is applied on different lines of the optical emission spectrum, which consists of atomic lines of argon, hydrogen, oxygen and nitrogen as well as molecular bands of N_2 and OH. The example given in figure 3 (d) shows the spatio-temporally resolved luminosity at the wavelength 337 nm, i.e. the most intensive band of the second positive system on N_2. In figure 3 (d) the tip of the needle electrode (cathode) is at 0 mm, while the horizontal line at 5 mm shows the end position of the quartz tube. The grounded electrode (anode) is located at 8.2 mm.

The discharge starts with a long lasting pre-phase ($t < 120$ ns, maximal emission in front of capillary) followed by ionization fronts propagating in different directions, as schematically shown by the arrows. At about 150 ns, the luminosity distribution of higher energetic transitions fills the gap completely and the plasma channels connect both

electrodes. Ten nanoseconds later the luminosity starts to decay and the filament phase ends followed by an afterglow.

4. NEEDLE-TO-PLANE DISCHARGE

The electrode configuration of the next discharge being discussed is similar to that one of the transient spark (see figure 4 (a)). It consists of a powered hollow electrode (syringe needle, outer diameter 2 mm, inner diameter 1.5 mm) and a copper plate ($2.5 \times 3.5\,\mathrm{cm}^2$) as the grounded electrode.

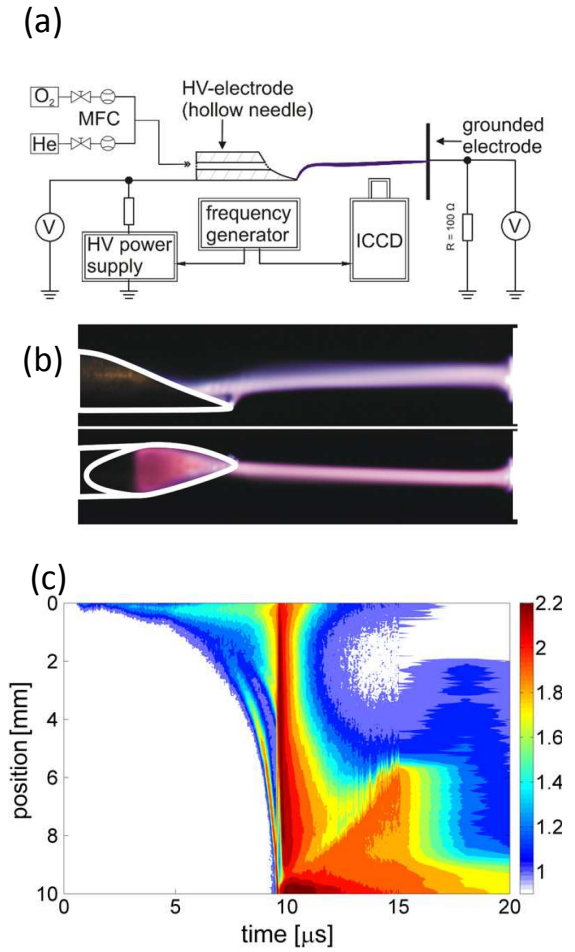

Fig. 4: Investigation of the needle-to-plane helium plasma: (a) Experimental set-up, (b) Photos of the discharge, (c) Contour plot obtained from phase-resolved optical emission spectroscopy [15].

The discharge is driven by a sinusoidal high-voltage with amplitudes between 2 and 10 $\mathrm{kV_{pp}}$ and 18 kHz frequency. The total current of the discharge is measured through a 100 Ω resistor and recorded by an 1 GHz digital oscilloscope (Tektronix DPO 7104) via voltage probes (Tektronix 6015A and P2220). Helium as the working gas is supplied through the needle electrode at a flow rate of 3 slm. Oxygen can be admixed to the helium gas.

Depending on the electrode gap width one or two current pulses per half-period of the sinusoidal high-voltage are observed. The current pulses appear on the leading edge of the voltage slope, its amplitude varies from 3 to 10 mA and its duration ranges from 10 and 18 µs (see [15] for details).

Since the discharge develops on a microsecond timescale with good reproducibility and very regular in phase with the applied voltage, short exposure time photos can be used to study the dynamic discharge evolution two-dimensionally resolved. Photos are captured by means of an ICCD camera (Stanford Computer Optics 4Picos-DIG) with a gate width of 10 ns and 2 ms accumulation time. The ICCD pictures are post-processed to obtain so-called contour plots which visualize the discharge development in the same manner as the streak or CCS images in the previous examples. These images give a continuous overview of the discharge development. Therefore, the intensity of each ICCD image is summarized over height, i.e. one dimension in space is reduced and the remaining data result in the intensity distribution over the length of the discharge gap. The contour plots are calculated by means of MATLAB using the *contourf*-function, i.e. data for irregular time steps can be interpolated. A result for 10 mm discharge gap and 3 $\mathrm{kV_{pp}}$ (one current pulse per half period with an amplitude of about 6 mA and a duration of about 30 µs) is shown in figure 4 (c).

The discharge development in figure 4 (c) can be divided in six phases. A glow starting to develop from the needle tip (anode) is obtained first. With time the intensity and the size of the glow increase, i.e. a plasma channel grows and expands towards the grounded electrode (phase 1). At 6.6 µs the head of the column separates from the channel and forms a first so-called forward bullet (phase 2). The primary channel, characterized by increasing intensity and spatial expansion, can be observed further on behind the bullet. At $t = 9$ µs a second forward bullet forms at the head of the column which is still connected to the needle tip. When the first bullet is close to the cathode, a back moving luminescence phenomenon is observed, the return stroke (phase 3), connecting both bullets at the head of the channel behind. The electrode gap is then bridged by a plasma column (phase 4). When this plasma column is in the near vicin-

ity of the plane electrode, a "glow-like" behavior of the discharge is seen and the maximum of the corresponding current pulse is reached (phase 5). Finally the plasma decays within about one microsecond while a plasma region expands from the cathode surface into the electrode gap (phase 6).
The general discharge behavior is almost identical in the negative voltage half-period. The direction of bullet propagation is reversed (so-called reverse bullets) since the formation and propagation of the plasma is not determined by the gas flow but by the electric field configuration. In case of a larger gap width (15 mm) a so-called pre-bullet is observed. This bullet also proceeds the first two phases but the discharge gap is not entirely bridged by the plasma channel. Several microseconds after this event a new column develops from the needle tip running through all six phases.

5. CONCLUSIONS

A short overview on the capabilities and peculiarities for the combined use of electrical, optical and spectroscopic diagnostics of filamentary plasma was given. The spatio-temporal development of single barrier microdischarges in nitrogen-oxygen gas mixtures operated by rectangular high voltage, a self-pulsing transient DC spark discharge and a sinusoidal operated needle-to-plane discharge have been studied by means of fast electrical, optical or spectroscopic methods. The techniques provide the necessary time resolution, are non-intrusive and give insights on the complex plasma morphology and its spatially and temporally resolved development.
In certain situations such methods enable the determination of plasma parameters. On the way to more reliable and controllable plasma sources such activities must be increased in connection with the application of other diagnostics giving further access to basic plasma parameters.

ACKNOWLEDGEMENT

These investigations were partly supported by the research cooperation "Campus PlasmaMed" endorsed by German Ministry of Education and Research (BMBF, grant no 13N11188) which is highly appreciated.

REFERENCES

[1] A. Fridman *Plasma Chemistry*, Cambridge University Press, 2008

[2] K.-D. Weltmann, E. Kindel, Th. von Woedtke, M. Hähnel, M. Stieber and R. Brandenburg, *"Atmospheric pressure plasma sources - prospective tools for plasma-medicine"*, Pure Appl. Chem. **80**, 1223-1237, 2010

[3] P. Bruggeman and R. Brandenburg, *"Atmospheric pressure discharge filaments and microplasmas: physics, chemistry and diagnostics"*, J. Phys. D: Appl. Phys. **46**, 464001, 2013

[4] M. Kettlitz, H. Höft, T. Hoder, S. Reuter, K.-D. Weltmann and R. Brandenburg, *"On the spatio-temporal development of pulsed barrier discharges: influence of duty cycle variation"*, J. Phys. D: Appl. Phys. **45** 245201, 2012

[5] S. Liu and M. Neiger, *"Excitation of dielectric barrier discharges by unipolar submicrosecond square pulses"*, J. Phys. D: Appl. Phys. **34**, 1632-8, 2001

[6] A. Pipa, J. Koskulics, R. Brandenburg and T. Hoder, *"The simplest equivalent circuit of a pulsed dielectric barrier discharge and the determination of the gas gap charge transfer"*, Rev. Sci. Instrum. **83**, 115112, 2012

[7] H. Höft, M. Kettlitz, T. Hoder, K.-D. Weltmann and R. Brandenburg, *"The influence of O_2 content on the spatio-temporal development of pulsed driven discharges in O_2/N_2 gas mixtures"*, J. Phys. D: Appl. Phys. **46**, 095202, 2013

[8] T. Shao, C. Zhang, Z. Yu, Z. Niu, H. Jiang, J. Xu, W. Li, P. Yan and Y. Zhou, *"Discharge characteristic of nanosecond-pulse DBD in atmospheric air using magnetic compression pulsed power generator"*, Vacuum **86**, 876-880, 2012

[9] H.-E. Wagner, K.V. Kozlov and R. Brandenburg In R. Hippler, H. Kersten, M. Schmidt and K.H. Schoenbach *Low Temperature Plasma Physics. Fundamental Aspects*

and Applications vol. 1, Weinheim: Wiley-VCH, 271-306, 2008

[10] R. Brandenburg, M. Bogaczyk, H. Höft, S. Nemschokmichal, R. Tschiersch, M. Kettlitz, L. Stollenwerk, T. Hoder, R. Wild, K.-D. Weltmann, J. Meichsner and H.-E. Wagner, *"Novel insights into the development of barrier discharges by advanced volume and surface diagnostics"*, J. Phys. D: Appl. Phys. **46**, 464015, 2013

[11] R. Bussiahn, R. Brandenburg, T. Gerling, E. Kindel, H. Lange, N. Lembke, K.-D. Weltmann, Th. von Woedtke and T. Kocher, *"The hairline plasma: An intermittent negative dc-corona discharge at atmospheric pressure for plasma medical applications"*, Appl. Phys. Lett. **96**, 143701, 2010

[12] T. Gerling, T. Hoder, R. Brandenburg, R. Bussiahn and K.-D. Weltmann, *"Influence of the capillary on the ignition of the transient spark discharge"*, J. Phys. D: Appl. Phys. **46**, 145205, 2013

[13] T. Gerling, T. Hoder, R. Brandenburg, R. Bussiahn and K.-D. Weltmann, *"On the spatio-temporal dynamics of a self-pulsed nanosecond transient spark discharge: a spectroscopic and electrical analysis"*, Plasma Sources Sci. Technol. **22**, 065012, 2013

[14] T. Gerling, R. Bussiahn, C. Wilke and K.-D. Weltmann, *"Time-resolved ion density determination by electrical current measurements in an atmospheric-pressure argon plasma"*, EPL **105**, 25001, 2014

[15] T. Gerling, A.V. Nastuta, R. Bussiahn, E. Kindel and K.-D. Weltmann, *"Back and forth directed plasma bullets in a helium atmospheric pressure needle-to-plane discharge with oxygen admixtures"*, Plasma Sources Sci. Technol. **21**, 034012, 2012